Instrumentation for Ultrasonic Transkull Visualization

WILLIAM A. ERDMANN, MEMBER, IEEE, FRANCIS J. FRY, SENIOR MEMBER, IEEE, KENNETH W. JOHNSTON, AND NARENDRA T. SANGHVI, MEMBER, IEEE

Abstract—**Instrumentation operating in the 0.5 to 1.0 MHz frequency range specifically designed for acoustic visualization of intracranial anatomy through the intact adult human skull is described. The instrumentation consists of a commercial *B*-mode scanner which has been extensively modified to enhance the reduced sensitivity and resolution inherent in such visualization schemes, as well as aid in the identification of intracranial anatomy. The instrumentation is described in three parts: a) the analog video system including transducers, pulsers, receiver, and associated circuitry; b) the digital video system which includes the analog-to-digital converter, signal processing for longitudinal and lateral resolution improvement, and the interface with the commercial unit; and c) the system for storing the scans and for overlaying the anatomical atlas information. Preliminary results of the use of this instrumentation to obtain transkull ultrasonic images are also presented.**

I. INTRODUCTION

THE POTENTIAL for acoustic visualization of intracranial anatomy through the intact adult human skull was shown to exist in previous reports from the Indianapolis Center for Advanced Research, Indianapolis, IN [1], [2], wherein the frequency dependent acoustical properties of the skull were described. Other studies have also indicated such potential using sector sanning [3] and phased array techniques [4]. At frequencies of 0.5 to 1 MHz, and with the transducer beam axis normal to the skull during scanning, ultrasonic energy passes through the skull with minimum spatial and temporal distortion [5]; however, loss of sensitivity and resolution associated with transmission loss and operating frequency, respectively, required the implementation of signal processing schemes to enhance the images obtained. A commercial *B*-mode contact scanner (Searle Pho-Sonic SM, *B*-Mode Ultrasound Scanner), chosen on the basis of the rugged construction of its scan arm and pedestal and its compatible registration architecture, was modified to meet the needs of transkull visualization and identification of internal brain structure. The additions and modifications to this instrument, shown in Fig. 1, may be divided into three major parts: a) the analog video system which includes the transducer, pulser, receiver and associated circuitry; b) the digital video system including conversion to the digital domain and longitudinal and lateral signal processing; and c) the system for storing the brain scans and overlaying the anatomical atlas to aid in interpretation. This instrumentation, and the preliminary transkull images obtained using this system, are the subjects of this paper.

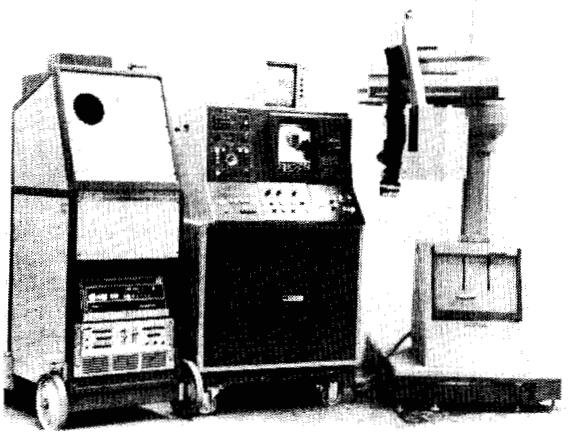

Fig. 1. Transkull visualization system showing, left to right, video overlay and storage system, modified Pho-Sonic main frame, and modified Searle Pho-Sonic scan arm and pedestal.

Manuscript received February 16, 1981; revised August 10, 1981. Portions of this paper were presented at the 24th Annual Meeting of the American Institute of Ultrasound in Medicine, Montreal, PQ, Canada, 1979.

W. A. Erdmann is with PTS Medrix, Bloomington, IN.

F. J. Fry and N. T. Sanghvi are with the Ultrasound Research Division, Indianapolis Center for Advanced Research, Inc., 410 Beauty Ave., Indianapolis, IN 46202.

K. W. Johnston is with the E Systems, Inc., Dallas, TX.

II. INSTRUMENTATION

A. Analog Video System

The analog video system was designed to 1) provide the low frequency acoustic signals necessary to penetrate the skull; 2) amplify received echoes to a level appropriate for digitization; 3) provide control of system gain; and 4) address the problems of sensitivity and, in part, of longitudinal and lateral resolution. The block diagram of the system is shown in Fig. 2. The transducers used in the transkull visualization system operate at frequencies in the 0.5 to 1.0 MHz range to avoid severe spatial and temporal distortion, as well as attenuation, evident at higher frequencies [5]. Specifically, three transducers operating at 0.5, 0.75, and 1.0 MHz have been fabricated for use with the system to achieve the greatest resolution permitted by the limiting sound transmission properties of the patient's skull. Each transducer, shown in Fig. 3, employs a flat 7.5-cm diameter lead metaniobate disc as the vibrating element, and is focused using an epoxy lens (focal distance of 18 cm) to yield lateral 3-dB beamwidths of 5.6, 4.6, and 4.7 mm, and axial 3-dB beamwidths of 8.5, 7.5, and 7 cm at 0.5, 0.75, and 1.0 MHz, respectively. Transducer acoustic outputs under normal operation (shown in Table I), as

0018-9537/82/0100-0005$00.75

TABLE I

Transducer Designation	Nominal Center Frequency (MHz)	Average Power (mW)	SPTA* Intensity ($mWcm^{-2}$)
TVT 43	0.5	2.2	5.8
TVT 44	0.75	35.0	150.0
TVT 45	1.0	8.8	40.0

*SPTA: Spatial peak/temporal average.

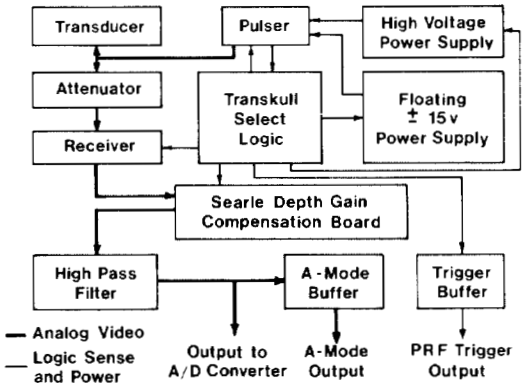

Fig. 2. Analog video system showing video train, select logic, and external outputs.

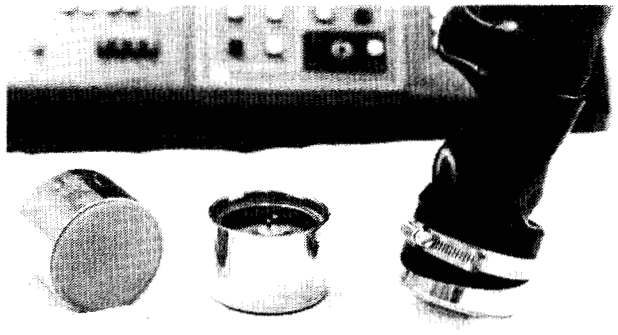

Fig. 3. Transducers designed for transkull visualization. Nominal center frequencies are, from left to right, 500 kHz, 750 kHz, and 1 MHz.

determined by measurements of total acoustic power using the radiation force method and transaxial beam plots, are in the range of most commercial units [6]. The variation in transducer output is normal in our experience for these large units.

The pulser starts the sequence of events in the video train by driving the transducer to produce an acoustic pulse. The capacitive-discharge pulser, based on the concepts described by Okyere and Cousin [7], is shown in block diagram form in Fig. 4. The trigger from the logic is amplified and inverted by the trigger circuit. Three silicon-controlled rectifiers, arranged in series to distribute the 1000-V supply, fire simultaneously to discharge capacitor C, which is rapidly recharged by a constant current source. R is an adjustable damping resistor. Fig. 5 shows the drive waveform produced by this pulser circuit and the received echo from an aluminum block.

The received acoustic signals are passed through an 82-dB variable high voltage attenuator (noncumulative accuracy of

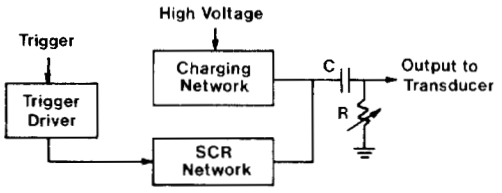

Fig. 4. Capacitive-discharge pulser.

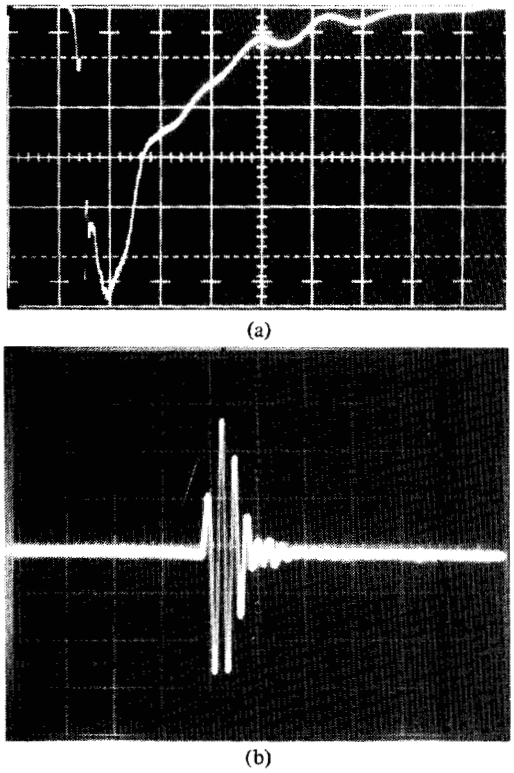

Fig. 5. (a) Output waveform of capacitive-discharge pulser driving 750-kHz transducer. Scales are 100 V/div and 1 μs/div. (b) Received echo from aluminum block at focus of transducer obtained from waveform in (a). Scales are 5 V/div and 2 μs/div.

±0.25 dB), thereby regulating system gain. The amount of attenuation is adjusted such that the dynamic range of the echoes may be matched to the dynamic range of the receiver. The attenuated acoustic signals are then passed on to the receiver, which contains several subsystems. A Ferranti ZN459T integrated circuit, selected for its excellent noise characteristics (3 μV root-mean-square (rms) in the pertinent frequency range) and 60-dB gain, serves as the receiver preamplifier. A diode protection network prevents destructive overdrive of the preamplifier, while reasonable recovery times (less than 200 μs) are achieved using a capacitively coupled 7-kΩ input impedance, with an external biasing network giving the capacitor a discharge path. By means of a 500-MHz relay, the output of the preamplifier may be switched to either a 20-dB linear amplifier or a 60 dB · V logarithmic amplifier. The receiver output is buffered by a line driver. Sensitivity for the completed receiver was measured at 10 μV rms, higher than would be expected with the preamplifier's noise specification, due to the nature of the diode protection and low impedance biasing networks. The frequency response of the receiver is flat to ±1 dB over a range from 437 kHz to 1.73 MHz. The

linear gain is 72 dB, and dynamic range 36 and 60 dB in the linear and logarithmic modes, respectively.

The output of the receiver passes through the depth gain compensation board of the commercial unit. At this point the commercial unit senses the presence of echoes and determines, on the basis of a level detector, whether to read from or write to the scan converter. The received acoustic signals pass from the depth gain compensation board to a 450-kHz high-pass filter and on to the analog-to-digital (A/D) converter. A buffer provides an analog video output that may be used for external signal processing.

The transkull select logic, also shown in Fig. 2, performs several functions, both in the analog video system to be discussed here and in the digital video system to be discussed later. One function of the logic is to switch from the commercial to the transkull system to allow accessibility to the original commercial configuration. The logic also supplies a pulse repetition frequency trigger to the pulser, as well as to a buffer, which provides an output from the machine for external signal processing. In addition, the logic allows selection of log or linear amplification in the receiver and also controls the routing of the signal through the depth gain compensation board of the commercial unit.

B. Digital Video System

The digital video system was designed to address the problems of inadequate longitudinal and lateral resolution, selection of the various transfer functions, and injection of transkull digital data into the digital data train. This system will be discussed in two parts. First, the general system will be described in conjunction with the logic that provides synchronization with the commercial digital system. This will be followed by a detailed description of significant blocks, including longitudinal and lateral processors, selectable transfer functions, and interface between the two digital systems.

A block diagram of the digital video system is shown in Fig. 6. The system clock is generated in the lateral processor, since the memory in the processor is controlled by a clock which must be synchronous with the system clock but four times higher in frequency. A 34.921-MHz communications crystal was selected for the lateral processor memory, yielding a 8.730-MHz system clock frequency. Besides serving as the transkull digital video system clock, the 8.730-MHz signal is inserted in place of the commercial unit's clock to assure synchronization of the two systems. As the two clock frequencies (8.752 and 8.730 MHz) differ by only 0.25 percent, no significant synchronization error is detectable.

The transkull select logic not only controls the insertion of the system clock into the commercial unit, but also performs other functions. It receives a pulse repetition frequency trigger from the commercial unit and routes it to the lateral processor and the pulser (Figs. 2 and 6). It also routes the appropriate digital data to the commercial unit's A/D converter output latch, depending on whether the transkull or the commercial system is selected.

Analog data are digitized by an 8-bit A/D converter at the system clock rate of 8.730 MHz (Fig. 6). The digital output is

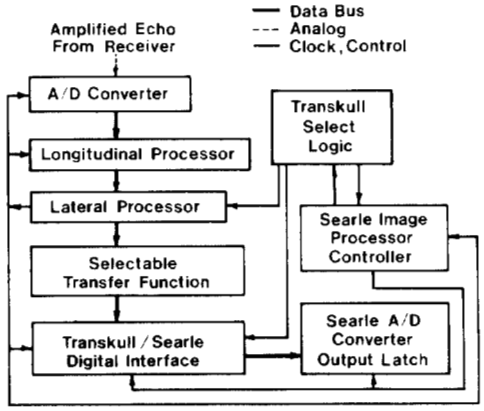

Fig. 6. Digital video system showing data train and select logic.

clocked into the longitudinal processor, a form of peak detector. Its output is clocked into the lateral processor, which compares three lines of data to determine peaks in the lateral direction. A look-up table in read-only memory (ROM) allows the selection of a variety of transfer functions. The processed data are then passed to the interface circuit and clocked into the A/D converter output latch of the commercial unit.

The longitudinal processor utilizes a digital peak detecting scheme based on the principle of deconvolution of the returned signals to resolve the impulse response at each target interface. By use of a well-described algorithm [8], [9], the returned echo signals can be written as

$$y(t) = \int h(t)\, x\,(t - T)\, dT \tag{1}$$

where $y(t)$ is the returned echo and $x(t)$ is the incident waveform; $h(t)$, the total impulse response of the system and tissue, is given by

$$h(t) = A_i \delta\,(t - t_i) \tag{2}$$

where $\delta\,(t - t_i)$ is the impulse response at time t_i, t being the time at which the reflection from the ith interface arrives, and A_i is the signal amplitude at t_i. Substituting (2) into (1), multiplying both sides by $x(t + T)$, and integrating over the entire time yields

$$R_{xy}(t) = A_i R_x(t - T) \tag{3}$$

where $R_{xy}(t)$ is the cross-correlation coefficient, $R_x(T)$ is the auto-correlation coefficient, and A_i is the signal strength.

Implementation of the above algorithm on a B-mode scanner is impractical because both auto-correlation and cross-correlation functions must be computed in the time between transducer excitations (1.33 ms for this unit). Therefore, a sliding window of 16 bytes is used instead of the whole signal string. A block diagram of the circuitry to implement this scheme is shown in Fig. 7. The digitized signals are converted to absolute values before processing. Two processors are available in the present system: a three-point and an adjustable 1–16-point sliding window comparator. In both, the center point amplitude is compared with neighboring points. If this amplitude is greater than the others, then the output register is enabled and the center data are stored. A boxcar circuit allows these data to be clocked out with a selectable pulsewidth.

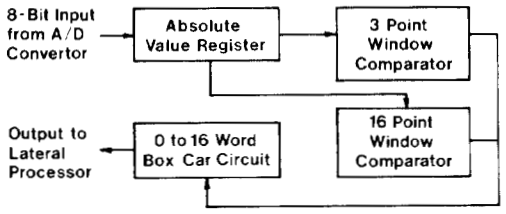

Fig. 7. Longitudinal processor.

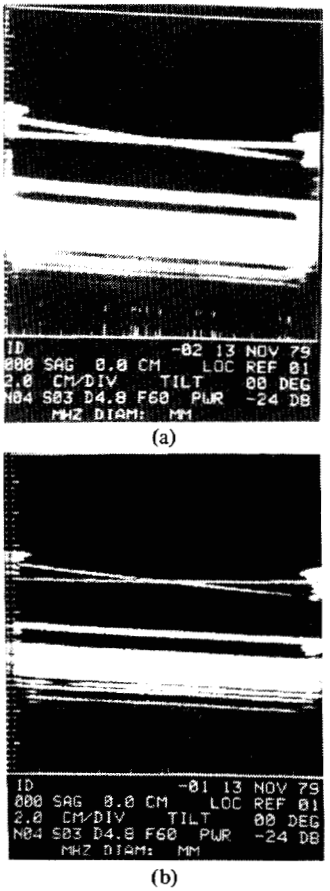

Fig. 8. Scan of converging 0.33-mm nylon strings using the 750-kHz transducer (a) without processing and (b) with processing.

Fig. 8 shows transkull (human cadaver skull) scans of converging 0.33-mm diameter nylon strings using the 750-kHz transducer without and with longitudinal processing (6-word). Without processing, the strings appear to merge at a point where the measured separation is 4 mm. With processing, the strings appear to merge at a point where the measured separation is 2 mm, demonstrating the ability of this processor to improve longitudinal resolution.

In order to improve the limited lateral resolution imposed by the low operating frequency of the transkull transducer, a lateral processor was developed which employs a form of peak detection by successively storing two scan lines of data and comparing parallel points along these lines with the line of incoming data. If the amplitudes at each point continuously increase or decrease between successive lines, the processor output is zero, but if the point amplitude of the center scan line is greater, the amplitude is retained. If there is no change in amplitude with position, the processor retains the output, allowing for the scanning of flat surfaces.

Though the basic processing scheme is conceptually simple, problems arise in implementation due to limitations in scan line density, as well as ambiguities in A/D conversion and longitudinal processing and jitter inherent in manual scanning. The memory must be able to store data at the system clock rate, but the number of data bits available is ultimately limited by economic considerations.

If the line density is too great, changes in signal amplitude cannot be adequately discriminated. If the line density is too small, lateral peaks and even small targets may be missed. The line density in a *B*-mode scanner is a function of scanning speed and pulse repetition frequency. Since the requirement of scanning normal to the skull to minimize attenuation and beam distortion will result in a highly variable scanning speed, the usefulness of this type of lateral processor for a fixed pulse repetition frequency is severely compromised. Fortunately, the commercial device provides the option of pulse repetition frequency as a function of scanning speed, and by scanning across a fixed distance at a number of speeds, a characteristic line density of 32 lines per centimeter with a variation of 20 percent was observed. Using this figure, the 6-bit depth of processor memory, and the average slope of the sides of the transducer's transaxial beam profile, it was clear that lateral signals with pressure amplitudes below 30 percent of the maximum displayed amplitude would not be adequately processed. Therefore, the unit was modified so that a selectable number of lines could be discarded, which effectively lowered line density and allowed adequate processing. For instance, if two of three lines are discarded, the line density becomes 11 lines per centimeter, so that echoes above 12 percent of the maximum displayed amplitude are processed.

A second problem with implementation of this scheme arises from the fact that parallel points in the scan line are processed (Fig. 9), but the data may not be parallel because of ambiguities in A/D conversion and longitudinal processing and jitter inherent in manual scanning. The boxcar circuit in the longitudinal processor (Fig. 7) helps solve this problem by allowing the duration of the peak detected signal to be several points (clock cycles) long. In addition, the lateral processor was designed to compare three points longitudinally as well as laterally, which results in a matrix that compares the center point *C* to the eight surrounding points (Fig. 9(b)).

A block diagram of the lateral processor is shown in Fig. 10. Memory is organized in a serpentine first-in/first-out structure. Upon receipt of a pulse repetition frequency trigger, 4096 bits are successively stored at the digital video system clock rate of 8.73 MHz. As each real-time 6-bit data byte is stored in memory block 1 and latch *U*, the first byte in memory block 2 is clocked out to latch *X*. When 4096 bytes have been stored in this fashion, the system shuts down until the next pulse repetition frequency trigger. Therefore, at any given time, latches *U*, *B*, and *X* contain parallel data bytes in three successive scan lines. Data bytes are simultaneously clocked from latches *U*, *B*, and *X* to latches *V*, *C*, and *Y*, respectively, then to *W*, *D*, and *Z*, to form the 3 × 3 matrix shown in Fig. 9(b). The data byte in latch *C* is compared to the bytes in the other latches

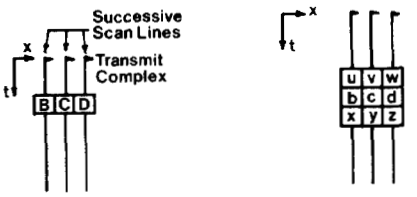

Fig. 9. Description of lateral processing scheme. (a) Parallel points in time from transmission of three successive scan lines. (b) 3 × 3 matrix actually processed.

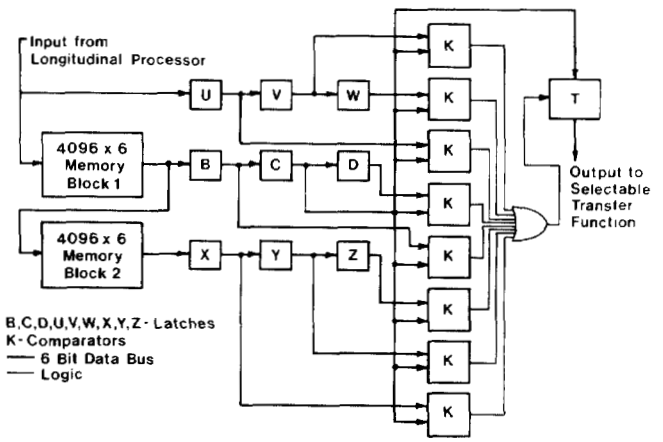

Fig. 10. Lateral processor.

by eight comparators, labeled *K* in Fig. 10. If any comparator finds a data byte greater than that in latch *C*, the OR gate resets transmission latch *T* to zero. Therefore, only when latch *C* contains a data byte greater than or equal to the bytes in the other latches are data available at the output of the processor. Transkull scans of two 0.33-mm strings spaced 4.5-mm apart without and with lateral processing are shown in Fig. 11.

The output of the lateral processor circuit is fed to an operator selectable variable transfer function circuit. The data form an address to a ROM (Fig. 12(a)) and map to data stored in the memory. By programming the ROM for particular functions and letting the three highest bits in the address be selectable by an external switch, different transfer functions can be obtained, ranging from log to linear to exponential functions (Fig. 12(b)). The output presently consists of 4 bits which are converted internally into ten discrete levels of output. A new ROM is being programmed for a full 6-bit output.

Fig. 13 shows a block diagram of the circuit that inserts transkull data into the commercial unit's digital data train. This insertion occurs at the output latch of the commercial unit's analog-to-digital converter so that the registration system of the commercial unit is retained intact. Besides simply selecting data from the appropriate data train, the interface circuit performs an important second function. As previously mentioned, the conversion rate for transkull data is 8.73 MHz. The commercial unit's conversion rate is synchronous with this rate but, depending on image field size, can be as much as four times slower; this allows transkull data to be missed by the commercial unit's conversion clock. To overcome this problem, the interface circuit stores a word of data, compares

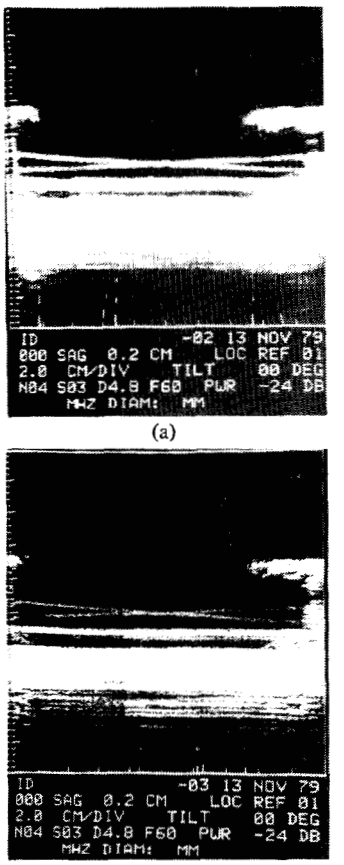

Fig. 11. Cross-sectional scan of converging 0.33-mm nylon strings at 4.5-mm spacing using the 750-kHz transducer with skull section strapped across face (a) without processing and (b) with processing.

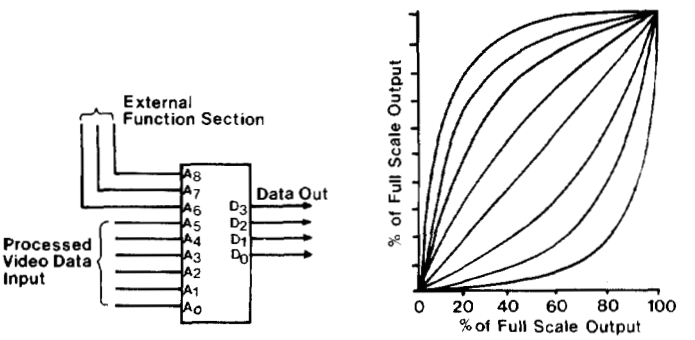

Fig. 12. Operator selectable variable transfer function read-only memory (a) and curves (b).

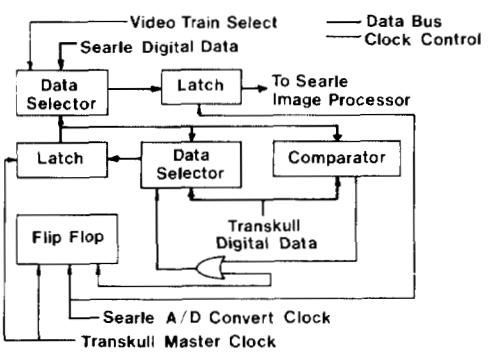

Fig. 13. Interface between transkull and Searle digital data trains.

it to the next incoming word, and stores the larger of the two. The process is repeated until the commercial unit's conversion clock latches the stored word into the A/D output latch. The next incoming transkull word is then automatically stored and the process repeats itself. Only in an extreme case is any transkull data discarded, i.e., longitudinal processor window of three sample intervals and boxcar circuit disabled. In all other cases, true data are discriminated from noise and retained until clocked out by the commercial unit's conversion clock. Of course, some spatial error occurs in this process, but the error is no more than 0.2 mm when the 10 X 10-cm image field size is selected.

C. *Video Overlay/Storage System*

A means of identifying internal cranial anatomy is incorporated into the video overlay/storage system shown in block diagram form in Fig. 14. An RCA TC1005 closed-circuit video camera is used to view an anatomical atlas placed on a sliding tray. A Fujinan CCTV zoom lens allows sizing of the atlas, and the tray permits overlay positioning. Mirrors are used to obtain the appropriate focal distance for the camera. The camera output may be mixed with a scan through a Panasonic special effects generator and displayed on the commercial unit's viewing monitor.

Because this type of analysis is most conveniently performed after the examination, a means of storing scans in video format is necessary. The Arvin/Echo VDR-1RA video discassette recorder selected for this function features still-frame image reproduction superior to reel-to-reel-type video recorders. The commercial unit's scan converter was selected as another temporary storage device because one cannot read from and write to the video disk simultaneously.

The video overlay/storage logic incorporates the timing and control circuits to write TV format video onto the scan converter tube. The system is first switched to the off-line mode, which inhibits the grid and test generation displayed in real time in the commercial unit's normal mode of operation. This circuit also switches to TV format sweeps so that the whole surface of the scan converter tube may be utilized for reading and writing. When the operator initiates a write command, the scan converter video input is switched to the video disk output. Sweep sync, normally derived from the commercial unit, is stripped from the video disk during this sequence because it is totally dependent on the physical position of the head in relation to the disk. After appropriate control signals are applied to the scan converter to allow the disk video to be written, overlays may be performed and stored on the video disk.

III. Preliminary Results

A horizontal scan of a 60-year-old volunteer male subject with presumed normal anatomy, taken with the 750-kHz transducer, longitudinal processor window of 16 samples, and linear transfer function, is shown in Fig. 15. Fig. 16 shows a horizontal scan of a 16-year-old female volunteer. Both Figs. 15 and 16 were made as a photographic mirror image since the hemisphere opposite the sound entry hemisphere is uncluttered with skull reverberation and other artifacts. The image processing being built into the final system will elimi-

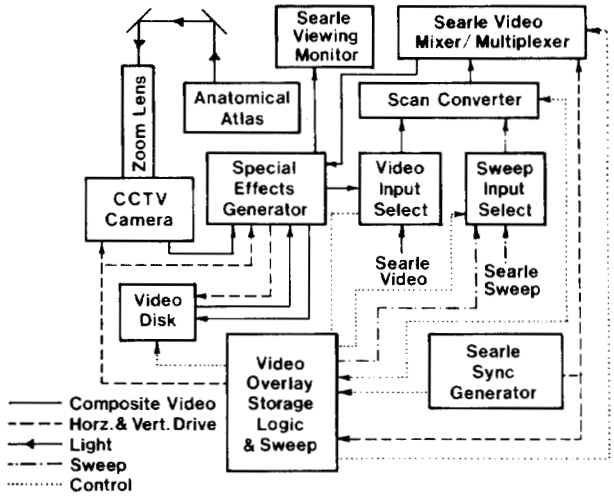

Fig. 14. Video overlay/storage system.

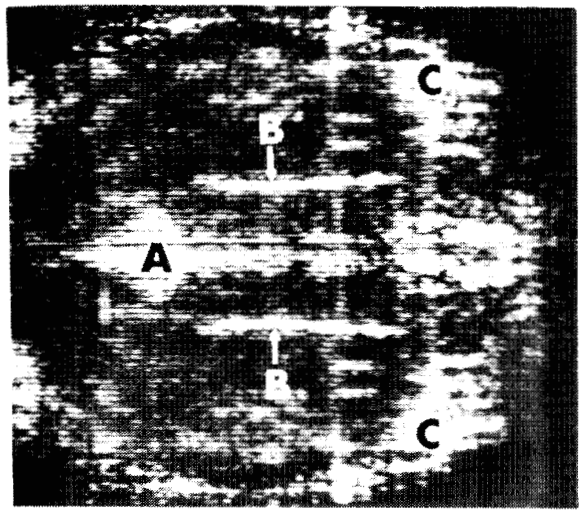

Fig. 15. Horizontal scan of 60-year-old male volunteer with presumed normal anatomy showing: (a) falx cerebri; (b) lateral ventricles; and (c) cranium. Scan was taken at a position some 60 mm above Frankfurt plane [10] showing nearly continuous midline reflection and roof of lateral ventricles.

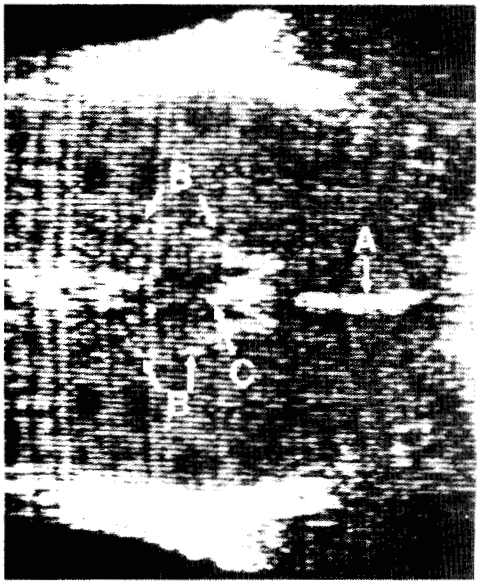

Fig. 16. Horizontal scan of 16-year-old female volunteer with presumed normal anatomy showing: (a) falx cerebri; (b) brain stem outline; and (c) cerebral aqueduct. Scan is approximately 25 mm above Frankfurt plane[10].

nate the need for photographic means to produce a full brain composite image.

The most effective means of acoustically coupling the instrument to the patient in terms of comfort, examination time, and transmission loss is under investigation, with water bath coupling currently employed. Proposed future developments include addition of a tissue characterization scheme based on the frequency dependence/ultrasonic backscatter, further real-time signal processing, and implementation of an image processing computer to enhance echographic visualization.

ACKNOWLEDGMENT

The authors wish to thank Dr. J. Timothy Patrick for his assistance in identifying anatomical structures in the transkull scans, and Dr. Stephen A. Goss.

REFERENCES

[1] F. J. Fry, "Transkull transmission of axisymmetric focused ultrasonic beams in the 0.5 to 1 MHz frequency range: Implications for brain tissue visualization, interrogation and therapy," in *Ultrasonic Tissue Characterization II*, National Bureau of Standards, Special Pub. No. 525, pp. 203–208, Apr. 1979.

[2] F. J. Fry, R. C. Eggleton, and R. F. Heimburger, "Transkull visualization of brain using ultrasound: An experimental model study," in *Ultrasonics in Medicine*, M. DeVlieger, D. N. White, and V. R. McCready, Eds. Amsterdam: Excerpta Medica, 1974, pp. 97–101.

[3] H. J. Freund, J. C. Somer, K. H. Dendel, and K. Voight, "Electronic sector scanning in the diagnosis of cerebrovascular disease and space occupying processes," *Neurology*, vol. 23, pp. 1147–1159, 1973.

[4] O. T. von Ramm, S. W. Smith, J. A. Kisslo, "Ultrasound tomography of the adult brain," in *Ultrasound in Medicine*, vol. 4, D. White and E. A. Lyons, Eds. New York: Plenum, 1976, pp. 261–267.

[5] F. J. Fry, and J. E. Barger, "Acoustical properties of the human skull," *J. Acoust. Soc. Am.*, vol. 63, pp. 1576–1590, 1977.

[6] P. L. Carson, P. R. Fischella, and T. V. Oughton, "Ultrasonic power and intensities produced by diagnostic ultrasound equipment," *Ultrasound Med. Biol.*, vol. 3, pp. 341–350, 1978.

[7] J. G. Okyere and A. J. Cousin, "The design of a high voltage SCR pulse generator for ultrasonic pulse echo applications," *Ultrason.*, vol. 17, pp. 81–84, 1979.

[8] A. C. Kak, L. R. Beaumont, and J. Wofley, "Signal processing in the determination of acoustic impedance profiles," Quarterly Progress Rep., NINCDS Contract NO1-NS-3-2319, 1974.

[9] A. C. Kak, F. J. Fry, and N. T. Sanghvi, "Acoustic impedance profiling: An experimental model and analytical study with implications for medical diagnosis," in *Ultrasound in Medicine*, vol. 2, D. White and R. Brown, Eds. New York: Plenum, 1976; pp. 477–488.

[10] A. Delmas and B. Pertuiset, *Cranio-Cerebral Topometry in Man*. Springfield, IL: Charles C. Thomas, 1959, p. 171.